# INTERACTION OF WAVES WITH $N$ VERTICAL CIRCULAR CYLINDERS

By Moo-Hyun Kim,[1] Member, ASCE

**ABSTRACT:** In this paper, the diffraction theory originally developed for $N$ bottom-mounted vertical circular cylinders is reviewed and generalized to be applicable to deep-draft truncated vertical cylinders, such as the columns of a tension-leg platform (TLP). More importantly, the complementary radiation problem for $N$ vertical circular cylinders is solved. Radiation potentials as well as added mass and wave damping for six-degree-of-freedom motions are obtained in closed forms. To demonstrate the usefulness of the present method, it is applied to the computation of wave loads and hydrodynamic coefficients for four columns of the ISSC TLP and a row of 19 bottom-mounted vertical cylinders. The present method quickly produces reasonably accurate solutions and precludes the laborious convergence test and grid generation, and hence should be a valuable tool for the preliminary design of deep-draft multicolumn structures, especially when the number of the columns is large.

## INTRODUCTION

A number of offshore structures, such as tension-leg platforms (TLPs) and deep-draft semisubmersibles, consist of vertical columns that are usually connected by horizontal pontoons at large depths (Demirbilek 1989). It is also actively considered to use this system as a large-scale offshore airport or work station. This kind of gigantic structure can have up to several hundred columns. As the size and number of the columns increase, the interaction between waves and arrays of columns becomes increasingly important. The resulting wave loads as well as free-surface elevation on these multicolumn structures can be surprisingly large due to a strongly reinforcing wave interaction. In a particular platform design, it is important to avoid these peaks, especially in an operational condition.

There exists extensive literature on the subject of linear wave interaction with multiple bodies (Spring and Monkmeyer 1974; Ohkusu 1974; Kagemoto and Yue 1986a), however most of them are limited to the diffraction problem, and the complementary radiation problem has rarely been studied (Chen and Molin 1990). Most notably, Kagemoto and Yue (1986) developed a powerful method that solves in principle all multiple-body diffraction problems where the solutions are already known for the individual elements. On the other hand, large-spacing approximate solutions (McIver and Evans 1983; Williams and Demirbilek 1988) have also been developed and shown to be efficient and fairly accurate when the cylinders are not closely spaced. Several attempts have also been made to investigate the second-order mean wave loads (Eatock et al. 1985; McIver 1987) as well as second-harmonic forces (Abul-Azm and Williams 1988; Chen and Molin 1990; Kim 1991) on multiple columns.

Recently, an explicit diffraction solution for arrays of bottom-mounted vertical circular cylinders, which is an extension of the earlier work by Spring

[1]Asst. Prof., Dept. of Civ. Engrg., Texas A&M Univ., College Station, TX 77843.

Note. Discussion open until May 1, 1994. To extend the closing date one month, a written request must be filed with the ASCE Manager of Journals. The manuscript for this paper was submitted for review and possible publication on February 3, 1992. This paper is part of the ***Journal of Waterway, Port, Coastal, and Ocean Engineering***, Vol. 119, No. 6, November/December, 1993. ©ASCE, ISSN 0733-950X/93/0006-0671/$1.00 + $.15 per page. Paper No. 3389.

and Monkmeyer (1974), has been obtained by Linton and Evans (1990). This analytic solution is a generalization of McCamy-Fuchs' solution to $N$ cylinders and expected to be an order of magnitude faster than any discretization-based numerical methods. This analytic solution is also expected to be very accurate at high frequencies, where other numerical methods need a large number of boundary or volume elements to have a reasonable accuracy at the expense of a substantial computing time.

In this paper, Linton and Evans' (1990) diffraction theory for $N$ bottom-mounted vertical cylinders is reviewed and extended to the complementary radiation problem. Analytical radiation potentials for six-degree-of-freedom motions of $N$ vertical cylinders are obtained. In contrast to the diffraction problem, there exist local (or evanescent) waves in the radiation problem, which makes relevant analyses more complicated. The explicit expressions for the added mass and wave damping are also obtained. All the diffraction and radiation solutions are generalized in order to be useful for the arrays of deep-draft truncated cylinders, such as the columns of a TLP.

## FORMULATION OF PROBLEM

We consider the linear interaction of monochromatic waves with arrays of $N$ bottom-mounted vertical circular cylinders. For analysis, Cartesian coordinate system $(x, y, z)$ as well as polar coordinate system $(r, \theta, z)$ with the origin on the mean free surface, and the $z$ axis positive upward is used. We also use $N$ local polar coordinate systems; $(r_j, \theta_j, z)$, $j = 1, \ldots, N$, which have origins at the centers of the $j$th cylinder $(X_j, Y_j, z = 0)$. The various geometric parameters relating to the relative positions of the $j$th and $k$th cylinders are shown in Fig. 1.

Assuming ideal fluid and small wave amplitude, we express the total first-order velocity potential $\Phi$ as a sum of incident, diffraction, and radiation potentials

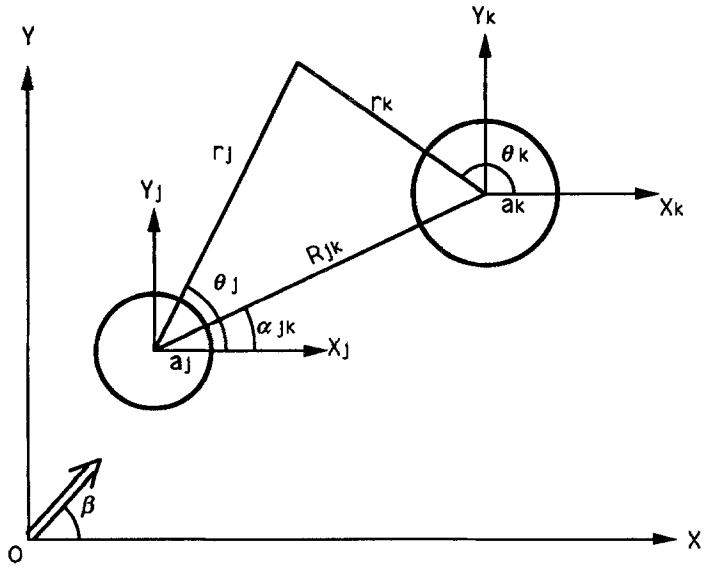


**FIG. 1. Coordinate System**

$$\Phi(x, t) = \Phi_I + \Phi_D + \Phi_R = \mathrm{R}_e[\phi(x)e^{-i\omega t}] \quad \ldots\ldots (1)$$

The diffraction potential $\Phi_D$ represents the scattered waves due to the presence of a fixed body, and radiation potential $\Phi_R$ represents radiated waves due to body motions.

**Wave Diffraction by Arrays of $N$ Vertical Columns**

In this section, we revisit the first-order diffraction problem of a regular incident wave in the presence of $N$ bottom-mounted vertical circular cylinders, which was considered in Linton and Evans (1990).

The incident monochromatic wave of amplitude $A$, wave heading $\beta$, and frequency $\omega$ has the form

$$\phi_I = -\frac{igA}{\omega} f_0(z)e^{ikr\cos(\theta-\beta)} = -\frac{igA}{\omega} f_0(z) \sum_{n=-\infty}^{\infty} i^n J_n(kr)e^{in(\theta-\beta)} \quad \ldots\ldots (2)$$

where wave number $k$ and frequency $\omega$ satisfy the dispersion relationship; $\omega^2 = k\mathrm{g} \tanh kh$ with g and $h$ being the gravitational acceleration and water depth, respectively. The depth attenuation function $f_0(z)$ is given by $f_0(z) = \cosh k(z + h)/\cosh kh$. The variable $J_n$ is the first-kind Bessel function of order $n$. Eq. (2) can be rewritten in terms of the local coordinate system of the $j$th cylinder

$$\phi_I = -\frac{igA}{\omega} f_0(z)\mathcal{J}_j e^{ikr_j\cos(\theta_j-\beta)}, \quad (\mathcal{J}_j = e^{ik(X_j\cos\beta + Y_j\sin\beta)}) \quad \ldots\ldots (3)$$

where $\mathcal{J}_j$ = phase factor associated with cylinder $j$.

The corresponding diffraction potential of the $j$th cylinder can be expressed in the form

$$\phi_D^j = -\frac{igA}{\omega} f_0(z) \sum_{n=-\infty}^{\infty} A_n^j Z_n^j H_n(kr_j)e^{in\theta_j} \quad \ldots\ldots (4)$$

The function $Z_n^j = J_n'(ka_j)/H_n'(ka_j)$, where $H_n$ = first-kind Hankel function of order $n$; and $a_j$ = radius of the $j$th cylinder. The notation $'$ denotes the derivative of a function. To solve for the unknown coefficients $A_n^j$, we first apply the following Graf's addition theorem for the Bessel functions to (4):

$$e^{in(\theta_j-\alpha_{jk})}H_n(kr_j) = \sum_{m=-\infty}^{\infty} J_{-m}(kr_k)H_{n-m}(kR_{jk})e^{-im(\alpha_{kj}-\theta_k)} \quad \ldots\ldots (5)$$

Then, we can rewrite the total scattering potential $\phi_S(=\Phi_I + \phi_D)$ in the form

$$\frac{\phi_S(r_k, \theta_k, z)}{-\frac{igA}{\omega} f_0(z)} = \sum_{n=-\infty}^{\infty} [\mathcal{J}_k J_n(kr_k)i^n e^{in(\theta_k-\beta)} + A_n^k Z_n^k H_n(kr_k)e^{in\theta_k}]$$

$$+ \sum_{j=1,\neq k}^{N} \sum_{n=-\infty}^{\infty} A_n^j Z_n^j \sum_{m=-\infty}^{\infty} e^{i(n-m)\alpha_{jk}}e^{-im(\pi-\theta_k)}J_{-m}(kr_k)H_{n-m}(kR_{jk}) \quad \ldots (6)$$

Upon applying the boundary condition on the $k$th cylinder; $\partial\phi_S/\partial r_k = 0$ on $r_k = a_k$, the coefficients $A_n^j$ can be determined from the following infinite systems of equations:

$$A_m^k + \sum_{j=1,\neq k}^{N} \sum_{n=-\infty}^{\infty} A_n^j Z_n^j e^{i(n-m)\alpha_{jk}} H_{n-m}(kR_{jk}) = -\mathcal{J}_k e^{im(\pi/2-\beta)}$$

$$(k = 1, \ldots, N, m = -\infty \sim \infty) \quad \ldots\ldots (7)$$

In order to evaluate $A_n^j$, the preceding infinite series with respect to $n$ needs to be truncated at $M$. Then, we solve the resulting matrix equation for $N(2M + 1)$ unknowns. The fast convergence of this series with $n$ has been observed in Linton and Evans (1990). After solving for the coefficients $A_n^j$, the first-order diffraction potential is explicitly given by (4).

Using (6) and (7), combined with Wronskian formula for Bessel functions, we can derive a simple expression of $\phi_S$ on the $k$th cylinder

$$\phi_S(a_k, \theta_k, z) = \frac{-2gA}{\pi\omega k a_k} f_0(z) \sum_{n=-\infty}^{\infty} \frac{A_n^k}{H_n'(ka_k)} e^{in\theta_k} \quad \ldots\ldots (8)$$

This simple expression is particularly useful in obtaining wave forces on each cylinder. The first-order wave loads are given by the integral

$$\begin{pmatrix} \mathbf{F}(t) \\ \mathbf{M}(t) \end{pmatrix} = \mathrm{R}_e \left[ \begin{pmatrix} \mathbf{F} \\ \mathbf{M} \end{pmatrix} e^{-i\omega t} \right] \qquad \begin{pmatrix} \mathbf{F} \\ \mathbf{M} \end{pmatrix} = i\rho\omega \int\int_{S_b} \phi_S \begin{pmatrix} \mathbf{n} \\ \mathbf{r} \times \mathbf{n} \end{pmatrix} dS \quad \ldots (9)$$

where $\rho$ = fluid density; $S_b$ = the mean body surface; $\mathbf{r} = (x, y, z)$ position vector; and $\mathbf{n} = (n_1, n_2, n_3)$ unit normal vector pointing into the body.

For deep-draft truncated cylinders, the fluid particle motions below the bottom of the cylinder are much smaller than those near the free surface, thus diffracted wave field by arrays of such cylinders can be reasonably well approximated by (3), (4), and (8). After integrating (8) over the body surface [e.g., performing $z$ integration from the bottom ($z = -D$) to the waterline of the cylinder], we obtain wave loads on a group of deep truncated cylinders. In case $D = h$, we can recover the exact solutions for the bottom-mounted cylinders.

The horizontal forces on the $j$th truncated cylinder of draft $D(>>1)$ can then be approximated by

$$\begin{pmatrix} F_x^j \\ F_y^j \end{pmatrix} = -\begin{pmatrix} i \\ 1 \end{pmatrix} \frac{2\rho g A}{k^2 H_1'(ka_j)} \frac{[\sinh kh - \sinh k(h - D)]}{\cosh kh} (A_{-1}^j \mp A_1^j) \quad .. (10)$$

The upper elements in the parentheses refer to the surge force and the lower elements to the sway force. Similarly, the pitch and roll moments are given by

$$\begin{pmatrix} M_x^j \\ M_y^j \end{pmatrix}$$

$$= \begin{pmatrix} 1 \\ -i \end{pmatrix} \frac{2\rho g A}{k^3 H_1'(ka_j)} \frac{[kD \sinh k(h - D) - \cosh kh + \cosh k(h - D)]}{\cosh kh}$$

$$(A_{-1}^j \pm A_1^j) \quad \ldots\ldots (11)$$

Finally, the yaw moment on the $j$th cylinder with respect to the global vertical axis can be obtained from

$$M_z^j = -Y_j F_x^j + X_j F_y^j \quad \ldots\ldots (12)$$

The total forces on the entire structure can be obtained by summing all the forces on each cylinder. There is no straightforward way to evaluate the vertical force by the present method, since the diffraction potential has been obtained only outside the radius of each cylinder. This will be further explained in the next section.

**Radiation Problem for Arrays of $N$ Vertical Columns**

In this section, Linton and Evans' (1990) diffraction formulation is extended to the corresponding radiation problem. In contrast to the previous diffraction problem, there exist local (evanescent) waves in radiation problem, which represent a standing wave system around a body. Wave numbers associated with such local waves can be found from the equation

$$\frac{\omega^2 h}{g} = -\kappa h \tan \kappa h \qquad \left(l - \frac{1}{2}\right)\pi \le \kappa_l h \le l\pi \qquad (l = 1, 2, \ldots) \quad \ldots (13)$$

For convenience, let us introduce a normalized radiation potential $\varphi_k$ for modes $k = 1$–$6$ (in order of surge, sway, heave, roll, pitch, and yaw), which represents the radiation potential for forced oscillation in $k$th mode with unit velocity. Then the total radiation potential has the form

$$\phi_R = \sum_{k=1}^{6} -i\omega\xi_k\varphi_k \quad \ldots (14)$$

where $\xi_k$ designates the amplitudes of six-degree-of-freedom body motions.

We next consider the simultaneous forced oscillation of $N$ vertical cylinders in a particular mode $i$. The radiation potential $\varphi_i$ of the $j$th cylinder can be written as a sum of progressing and local (evanescent) waves

$$\varphi_i^j = \sum_{n=-\infty}^{\infty} \left( B_n^j f_0(z) \frac{H_n(kr_j)}{kH_n'(ka_j)} + \sum_{l=1}^{\infty} L_{nl}^j f_l(z) \frac{K_n(\kappa_l r_j)}{\kappa_l K_n'(\kappa_l a_j)} \right) e^{in\theta_j} \quad \ldots (15)$$

where $K$ = modified Bessel function of the second kind; and the depth function for local waves $f_l(z) = \cos \kappa_l(z + h)/\cos \kappa_l h$. It is well known that the eigenfunctions $f_l(z)$, $l = 0, 1, 2, \ldots$, satisfy the orthogonality relation ($\int_{-h}^{0} f_l(z) f_m(z)\, dz = 0$ if $m \neq l$). To solve for the unknown coefficients $B_n^j$ and $L_{nl}^j$, we need to rewrite (15) using Graf's addition theorem. The propagating wave term with wave number $k$ can be treated exactly in the same manner as in the previous section. For local waves, we use the following addition theorem:

$$e^{in(\theta_j - \alpha_{jk})} K_n(\kappa_l r_j) = \sum_{m=-\infty}^{\infty} I_{-m}(\kappa_l r_k) K_{n-m}(\kappa_l R_{jk}) e^{-im(\alpha_{kj} - \theta_k)} \quad \ldots (16)$$

where $I$ = first-kind modified Bessel function. Then, we can rewrite (15) with respect to the local coordinate system of the $k$th cylinder as follows:

$$\varphi_i(r_k, \theta_k, z) = \sum_{n=-\infty}^{\infty} \left( B_n^k f_0(z) \frac{H_n(kr_k)}{kH_n'(ka_k)} + \sum_{l=1}^{\infty} L_{nl}^k f_l(z) \frac{K_n(\kappa_l r_k)}{\kappa_l K_n'(\kappa_l a_k)} \right) e^{in\theta_k}$$

$$+ \sum_{j=1, \neq k}^{N} \sum_{n=-\infty}^{\infty} \sum_{m=-\infty}^{\infty} \left( B_n^j f_0(z) \frac{J_m(kr_k)}{kH_n'(ka_j)} e^{i(n-m)\alpha_{jk}} H_{n-m}(kR_{jk}) \right.$$

$$+ \sum_{l=1}^{\infty} L_{nl}^{j} f_l(z) \frac{I_m(\kappa_l r_k)}{\kappa_l K_n'(\kappa_l a_j)} e^{i(n-m)\alpha_{jk}} e^{-im\pi} K_{n-m}(\kappa_l R_{jk}) \Bigg) e^{im\theta_k} \quad \ldots\ldots\ldots (17)$$

The normalized radiation potential $\varphi_i$ satisfies the following body-boundary condition on the $k$th cylinder:

$$\frac{\partial \varphi_i}{\partial r_k} = \begin{pmatrix} -n_i(-D \le z \le 0) \\ 0(z < -D) \end{pmatrix} \qquad (i = 1\text{–}6) \quad \ldots\ldots\ldots\ldots\ldots\ldots (18)$$

where, for convenience, the definition $\mathbf{r} \times \mathbf{n} = (n_4, n_5, n_6)$ is used. Here, we artificially enforce the boundary condition below the cylinder bottom to apply (17) to the truncated cylinder of draft $D >> 1$. After applying (18) and exploiting the orthogonality of depth functions $f_l(z)$, $(l = 0, 1, 2, \ldots)$, we obtain the following infinite systems of equations for $B_n^j$ and $L_{nl}^j$:

$$B_m^k + \sum_{j=1, \neq k}^{N} \sum_{n=-\infty}^{\infty} B_n^j \frac{J_m'(ka_k)}{H_n'(ka_j)} e^{i(n-m)\alpha_{jk}} H_{n-m}(kR_{jk}) = R_{mi}^k \mathsf{g}_0^i(h) \quad \ldots\ldots (19)$$

$$L_{ml}^k + \sum_{j=1, \neq k}^{N} \sum_{n=-\infty}^{\infty} L_{nl}^j \frac{I_m'(\kappa_l a_k)}{K_n'(\kappa_l a_j)} e^{i(n-m)\alpha_{jk}} e^{-im\pi} K_{n-m}(\kappa_l R_{jk}) = R_{mi}^k \mathsf{g}_l^i(h)$$

$$(k = 1, \ldots, N,\ m = -\infty \sim \infty,\ 1 \le l \le \infty) \quad \ldots\ldots\ldots\ldots\ldots (20)$$

where the right-hand-side term $R_{mi}^k$ for mode $i$ is given by

$$R_{mi}^k = \frac{1}{2} \delta_{\pm 1, m} \qquad (\text{for } i = 1, 5) \quad \ldots\ldots\ldots\ldots\ldots\ldots\ldots (21a)$$

$$R_{mi}^k = \frac{-mi}{2} \delta_{\pm 1, m} \qquad (\text{for } i = 2, 4) \quad \ldots\ldots\ldots\ldots\ldots\ldots\ldots (21b)$$

$$R_{m6}^k = X_k R_{m2}^k - Y_k R_{m1}^k \quad \ldots\ldots\ldots\ldots\ldots\ldots\ldots\ldots\ldots (21c)$$

with $\delta_{i,j}$ = Kronecker delta function. The depth functions $\mathsf{g}_0^i(h)$ and $\mathsf{g}_l^i(h)$ are given, respectively, by

$$\mathsf{g}_0^i(h) = \frac{4 \cosh kh[\sinh kh - \sinh k(h - D)]}{2kh + \sinh 2kh} \qquad \text{for } i = 1, 2, 6 \quad \ldots (22)$$

$$\mathsf{g}_0^i(h) = \frac{4 \cosh kh[kD \sinh k(h - D) + \cosh k(h - D) - \cosh kh]}{k(2kh + \sinh 2kh)}$$

$$\text{for } i = 4, 5 \quad \ldots\ldots\ldots\ldots\ldots\ldots\ldots\ldots\ldots\ldots\ldots\ldots\ldots\ldots (23)$$

$$\mathsf{g}_l^i(h) = \frac{4 \cos \kappa_l h[\sin \kappa_l h - \sin \kappa_l(h - D)]}{2\kappa_l h + \sin 2\kappa_l h} \qquad \text{for } i = 1, 2, 6 \quad \ldots\ldots (24)$$

$$\mathsf{g}_l^i(h) = \frac{4 \cos \kappa_l h(\kappa_l D \sin \kappa_l(h - D) - \cos \kappa_l(h - D) + \cos \kappa_l h)}{\kappa_l(2\kappa_l h + \sin 2\kappa_l h)}$$

$$\text{for } i = 4, 5 \quad \ldots\ldots\ldots\ldots\ldots\ldots\ldots\ldots\ldots\ldots\ldots\ldots\ldots\ldots (25)$$

To evaluate the unknown coefficients $B_m^k$ and $L_{ml}^k$, we need to truncate (19) and (20) at $n = M$ and $l = L$ to obtain $L + 1$ sets of $N(2M + 1)$ systems of equations. Using (17), (19), and (20), we can derive a simple

expression of $\varphi$ on the $k$th cylinder, which is very useful in deriving the formula for the added mass and wave damping

$$\varphi_i(a_k, \theta_k, z) = \sum_{n=-\infty}^{\infty} \left( f_0(z)\varphi_{ni}^k + \sum_{l=1}^{\infty} f_l(z)\varphi_{nli}^k \right) e^{in\theta_k} \quad \text{..... (26a)}$$

$$\varphi_{ni}^k = \frac{1}{k}\left\{ B_n^k \left[ \frac{H_n(ka_k)}{H_n'(ka_k)} - \frac{J_n(ka_k)}{J_n'(ka_k)} \right] + \mathsf{g}_0^i(h) R_{ni}^k \frac{J_n(ka_k)}{J_n'(ka_k)} \right\} \quad \text{..... (26b)}$$

$$\varphi_{nli}^k = \frac{1}{\kappa_l}\left\{ L_{nl}^k \left[ \frac{K_n(\kappa_l a_k)}{K_n'(\kappa_l a_k)} - \frac{I_n(\kappa_l a_k)}{I_n'(\kappa_l a_k)} \right] + \mathsf{g}_l^i(h) R_{ni}^k \frac{I_n(\kappa_l a_k)}{I_n'(\kappa_l a_k)} \right\} \quad \text{..... (26c)}$$

Recalling the fact that the added mass $\mu$ and wave damping $b$ are in phase with the acceleration and velocity of a body, respectively, they can be calculated from (26) and the following integral:

$$\mu_{ij} + i\frac{b_{ij}}{\omega} = \rho \int\int_{S_b} \varphi_i n_j \, dS \quad \text{..... (27)}$$

where $\mu_{ij}(b_{ij})$ represents the added mass (wave damping) in direction $j$ due to a sinusoidal motion of unit amplitude in the direction $i$. After performing the preceding integral, the added mass and wave damping of the $k$th cylinder for mode $i$ are given by

$$\mu_{ii} + i\frac{b_{ii}}{\omega} = \sum_{n=\pm 1} \left( \varphi_{ni}^k Q_i + \sum_{l=1}^{\infty} \varphi_{nli}^k Q_{li} \right) \pi c_i a_k \qquad (\text{for } i = 1, 2, 4, 5)$$

..... (28)

$$\mu_{66} + i\frac{b_{66}}{\omega} = \sum_{n=\pm 1} \left( (X_k \varphi_{n2}^k c_2 - Y_k \varphi_{n1}^k c_1) Q_1 \right.$$

$$\left. + \sum_{l=1}^{\infty} (X_k \varphi_{nl2}^k c_2 - Y_k \varphi_{nl1}^k c_1) Q_{l1} \right) \pi a_k \quad \text{..... (29)}$$

where $c_1, c_5 = 1$ and $c_2, c_4 = in\pi$. The depth-related functions in (28) and (29) are given by

$$Q_i = \frac{\sinh kh - \sinh k(h - D)}{k \cosh kh} \qquad (\text{for } i = 1, 2, 6) \quad \text{..... (30)}$$

$$Q_i = \frac{kD \sinh k(h - D) - \cosh kh + \cosh k(h - D)}{k^2 \cosh kh} \qquad (\text{for } i = 4, 5)$$

..... (31)

$$Q_{li} = \frac{\sin \kappa_l h - \sin \kappa_l (h - D)}{\kappa_l \cos \kappa_l h} \qquad (\text{for } i = 1, 2, 6) \quad \text{..... (32)}$$

$$Q_{li} = \frac{\kappa_l D \sin \kappa_l (h - D) + \cos \kappa_l h - \cos \kappa_l (h - D)}{\kappa_l^2 \cos \kappa_l h} \qquad (\text{for } i = 4, 5)$$

..... (33)

The preceding equations (28)–(33) can be used for the approximate eval-

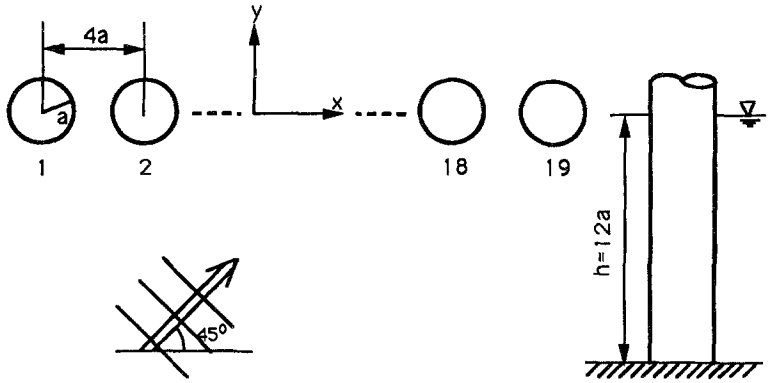


**FIG. 2. Array of 19 Bottom-Mounted Vertical Legs in Oblique Waves**

uation of the hydrodynamic coefficients of $N$ deep-truncated cylinders. When $D = h$, (26), (28), and (29) can be used as exact radiation solutions for $N$ bottom-mounted cylinders. As was pointed out earlier, we are unable to determine the heave-added mass and wave damping directly by the present method. This will be further discussed in the next section.

## NUMERICAL RESULTS AND ANALYSIS

The validity of the formula derived in previous sections is demonstrated through comparison with other numerical methods. The convergence of the present solutions with increasing numbers of Fourier components $M$ and local waves $L$, is fast. The choice of $M = 6$ and $L = 8$ gives sufficient accuracy and is used for all the results presented in this paper. It is worth noting that more local wave terms need to be included as water depth increases (Kim 1991).

The diffraction and radiation solutions derived in previous sections are exact solutions for arrays of bottom-mounted vertical cylinders. For illustration, we compute the surge and sway forces on 19 bottom-mounted identical cylinders arranged in one line in oblique incident waves ($\beta = 45°$), as shown in Fig. 2. Surge and sway forces on each cylinder in this case are calculated and compared with Kagemoto and Yue (1986b), where the full interaction method combined with a hybrid finite element program is used. In Fig. 3, we see excellent agreement between them. The wave-load calculation on large number of vertical cylinders can easily be treated by the present method, as shown in this example.

Although the equations are originally developed for arrays of bottom-mounted cylinders, it is applicable to deep-draft truncated vertical cylinders in view of the fact that the fluid-particle motions attenuate exponentially with depth. Therefore, we expect that wave loads on and diffracted wave field of deep-draft truncated cylinders can be well predicted by the present method. Based on this assumption, the modified formula for truncated cylinders was derived in previous sections. For illustration, wave loads on four identical columns (radius $a = 8.44$ m, draft $D = 35$ m, center-to-center spacing $L = 86.25$ m, and water depth $h = 200$ m) of the ISSC TLP (Eatock et al. 1986) are calculated for three wave headings ($\beta = 0°$, 22.5°, and 45°), and the results are compared with those computed from a three-

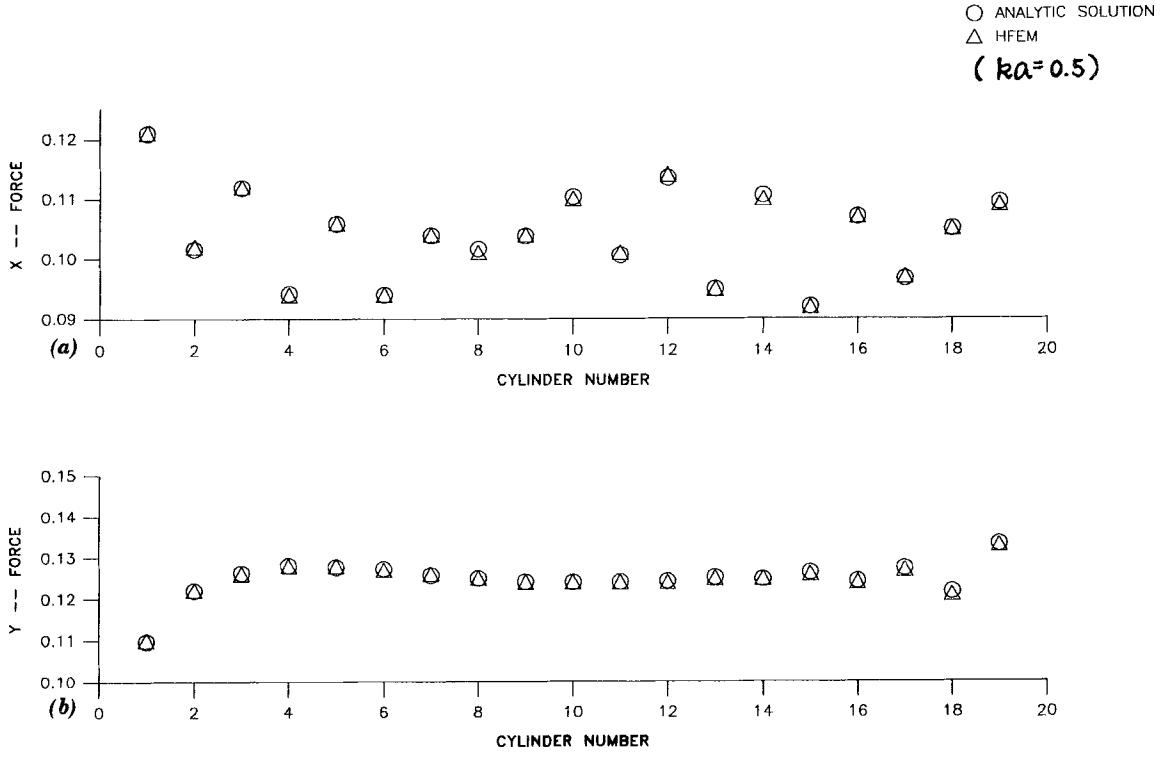


**Fig. 3. Surge and Sway Forces ($F/\pi\rho g a h A$) on Each of 19 Bottom-Mounted Vertical Cylinders in Oblique Waves ($\beta$ = 45°)**

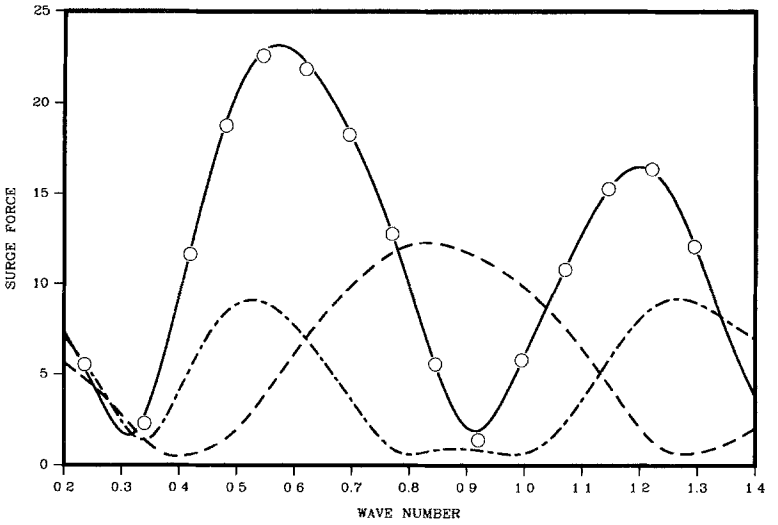


**FIG. 4. Surge Forces ($F/\rho g a^2 A$) on Four Columns of ISSC TLP as Functions of Nondimensional Wave Number $ka$: (——) $\beta$ = 0°; (---) $\beta$ = 22.5°; and (----) $\beta$ = 45°; (○ BEM)**

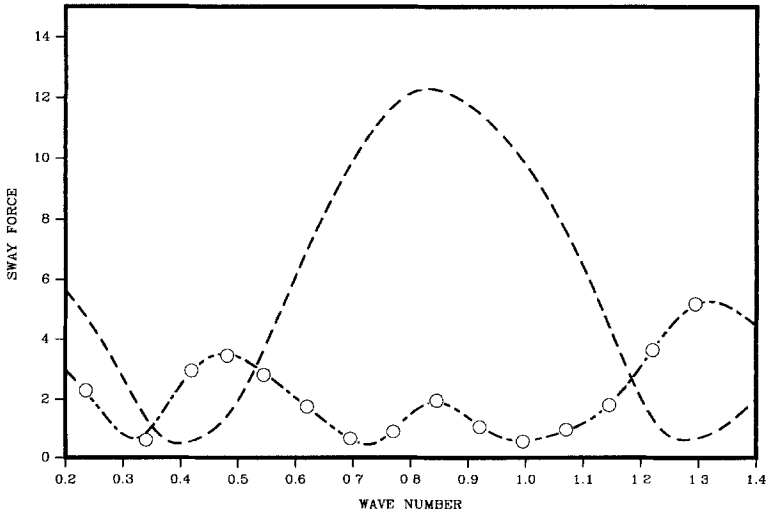


**FIG. 5. Sway Forces ($F/\rho g a^2 A$) on Four Columns of ISSC TLP as Functions of Nondimensional Wave Number $ka$: (——) $\beta$ = 22.5°; and (----) $\beta$ = 45°; (○ BEM)**

dimensional boundary element method (BEM) (Korsmeyer et al. 1988) in which four cylinders are discretized by 1,920 total quadrilateral elements.

It is seen in Figs. 4–9 that reliable results for surge-sway, pitch-roll, and yaw excitations can be obtained by the present method even at low frequencies, where the presence of the bottom of the cylinder can be felt. As pointed out earlier, the present method is not directly applicable to the

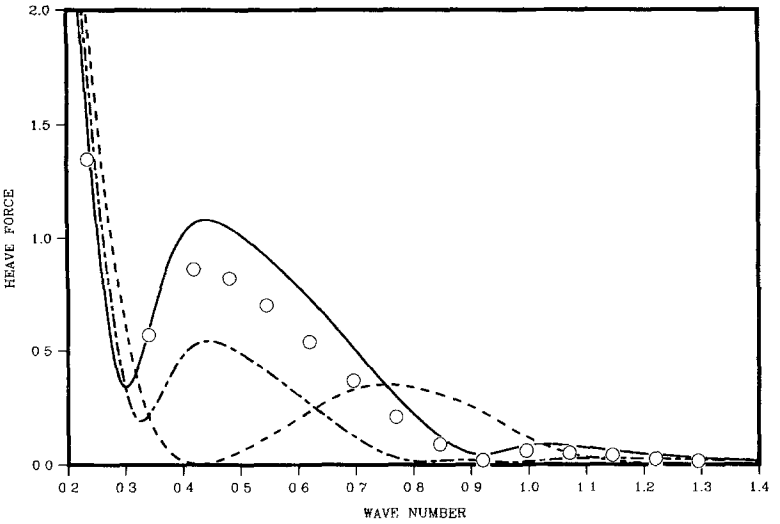


**FIG. 6. Heave Forces ($F/\rho g a^2 A$) on Four Columns of ISSC TLP as Functions of Nondimensional Wave Number $ka$: (——) $\beta$ = 0°; (– – –) $\beta$ = 22.5°; and (- - - -) $\beta$ = 45°; (○ BEM)**

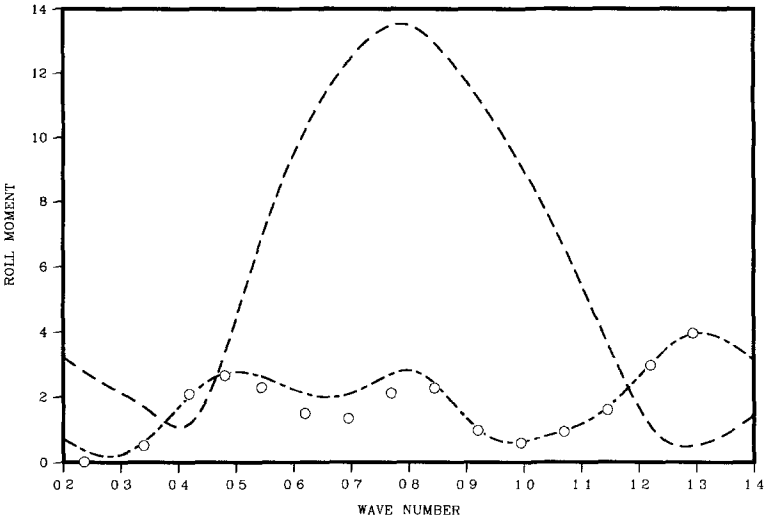


**FIG. 7. Roll Moments ($M/\rho g a^3 A$) on Four Columns of ISSC TLP as Functions of Nondimensional Wave Number $ka$: (– – –) $\beta$ = 22.5°; and (- - - -) $\beta$ = 45°; (○ BEM)**

computation of the heave force, which is expected to be small anyway for deep-draft columns. For heave-force computation, averaged peripheral bottom pressure times bottom area of the cylinder is used, and reasonable results are obtained in this way. These bottom pressures also influence the pitch-roll moments through the corresponding moment arms (Faltinsen and Demirbilek 1989). To account for this bottom effect more accurately, ei-

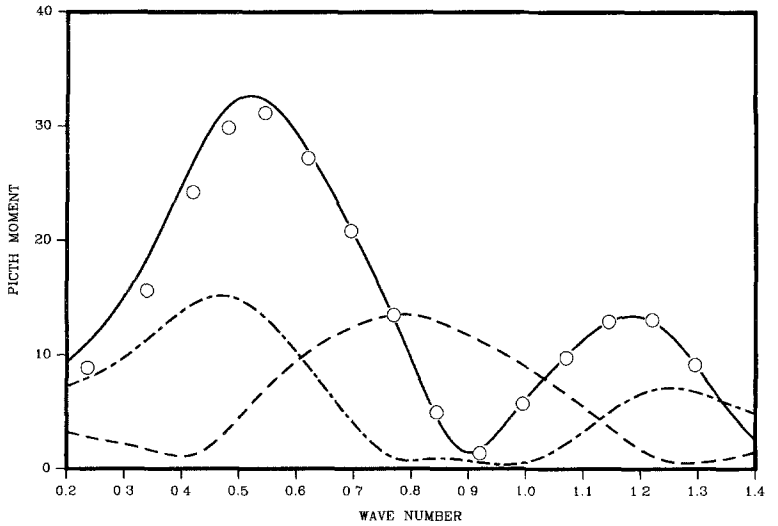


**FIG. 8. Pitch Moments ($M/\rho g a^3 A$) on Four Columns of ISSC TLP as Functions of Nondimensional Wave Number $ka$: (——) $\beta$ = 0°; (---) $\beta$ = 22.5°; and (----) $\beta$ = 45°; (○ BEM)**

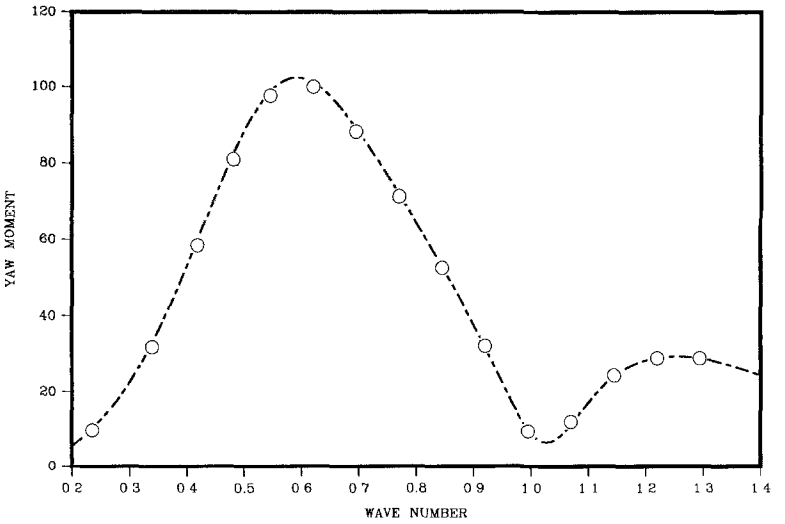


**FIG. 9. Yaw Moments ($M/\rho g a^3 A$) on Four Columns of ISSC TLP as Functions of Nondimensional Wave Number $ka$: (---) $\beta$ = 22.5°; (○ BEM)**

genfunction expansions may be used inside the radius of each cylinder (Williams and Demirbilek 1988).

In Figs. 4–9, we see pronounced peaks and troughs, which are closely associated with wave-phase effects among individual members. Ignoring wave-diffraction effects, the cancellation frequencies of the surge force for

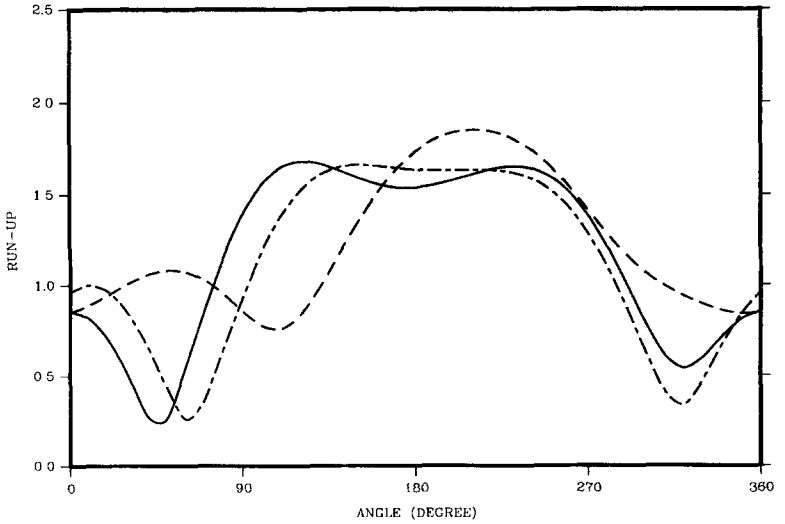


**FIG. 10. Wave Run-Up $|\eta/A|$ around Leg No. 1 for Wave Number $ka$ = 0.8: (——) $\beta$ = 0°; (---) $\beta$ = 22.5°; and (----) $\beta$ = 45°**

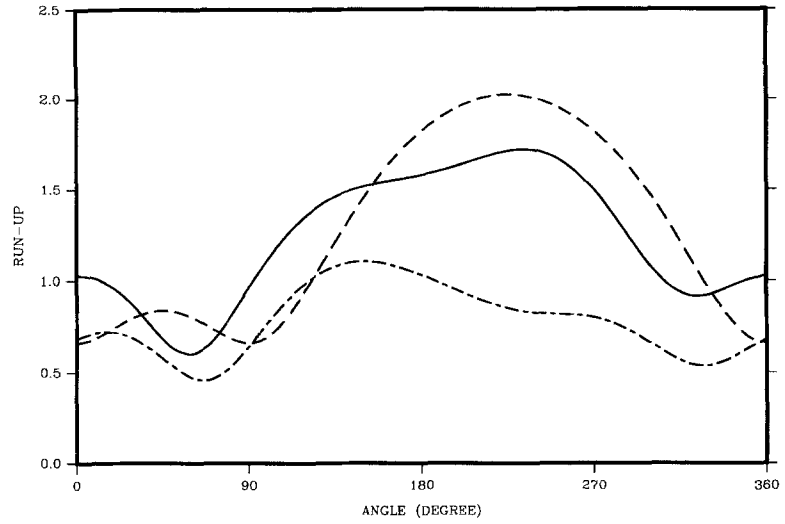


**FIG. 11. Wave Run-Up $|\eta/A|$ around Leg No. 2 for Wave Number $ka$ = 0.8: (——) $\beta$ = 0°; (---) $\beta$ = 22.5°; and (----) $\beta$ = 45°**

$\beta$ = 0, for example, can be found from $\cos kL/2 = (2n - 1)\pi/2 (n = 1, 2, \ldots)$. According to this, the cancellation frequency occurs at $ka$ = 0.31, 0.92, . . . for the given geometry, which coincides well with the result given in Fig. 4. It is seen in Figs. 4–9 that wave loads are very sensitive to the change not only in wavelength but also in wave headings. It is of interest to see that the maximum surge force for $\beta$ = 45° is greater than that for $\beta$ = 22.5°. Heave forces are very small, as expected, compared to the other

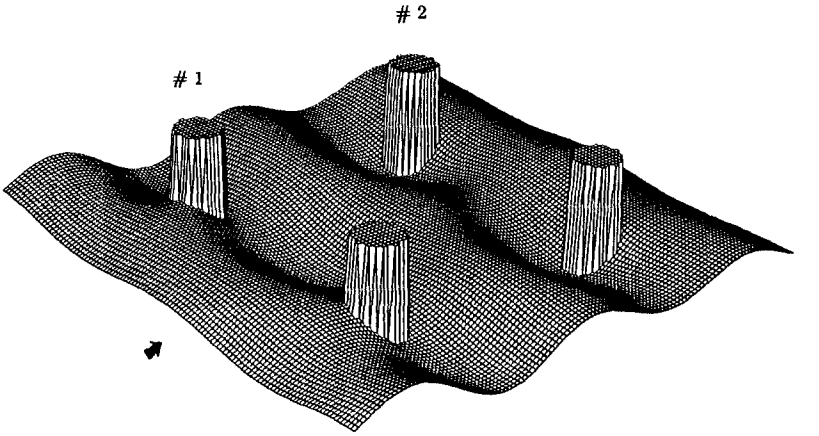


**FIG. 12. Free-Surface Elevation ($\eta/A$) around ISSC TLP for Wave Number $ka$ = 0.8**

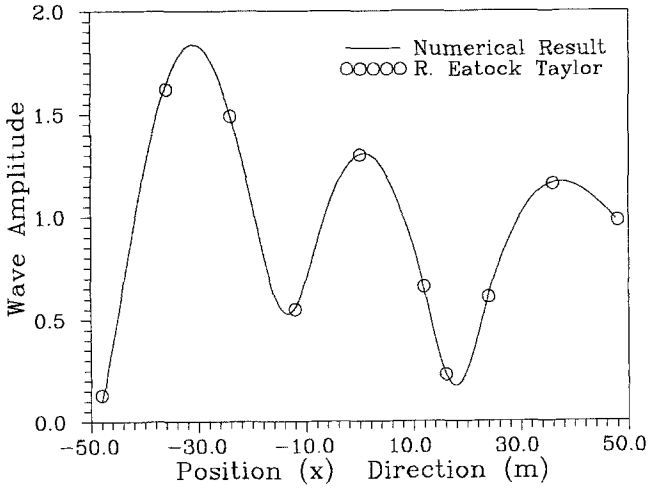


**FIG. 13. Relative Wave Amplitude along the $x$-axis for Four Columns**

forces, and attenuate rapidly with wave frequency. In Figs. 4–9, circles represent the results computed from the three-dimensional panel program.

In Figs. 10 and 11, the wave run-up around no. 1 and no. 2 columns (see Fig. 12) is plotted for wave number $ka$ = 0.8 and three different incident wave angles. Due to the interaction between columns, run-up profile of each cylinder is quite different from that of a single cylinder (Kim and Yue 1989). In most cases, we observe maximum wave run-up at the weather side of each cylinder. The "bird-eye" view of the free-surface elevation around the four columns is presented in Fig. 12. This kind of computation is particularly required to determine the air gap (deck height) of the offshore platforms (Demirbilek 1989) and can be routinely carried out by the present method.

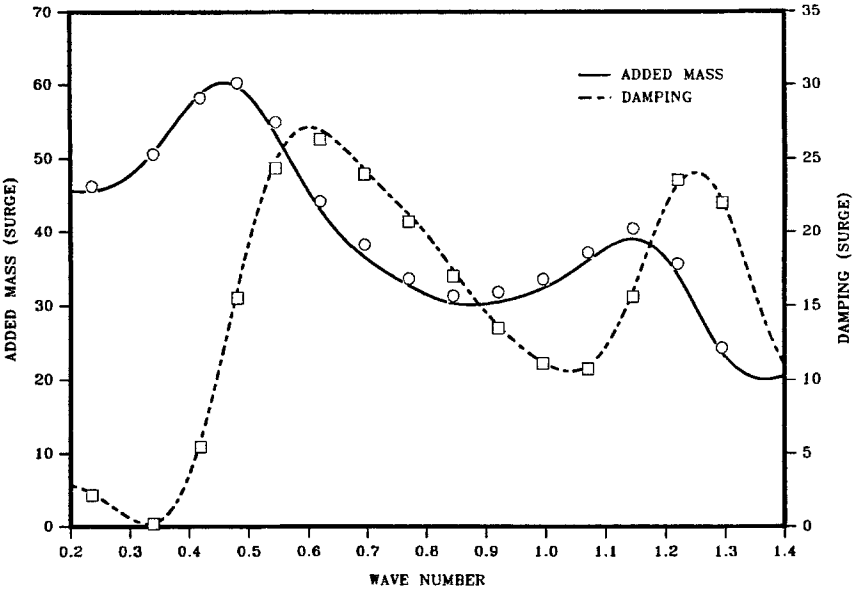


**FIG. 14. Surge-Added Mass ($\mu_{11}/\rho a^3$; ——) and Wave Damping ($b_{11}/\rho a^3\omega$; ----) for Four Columns of ISSC TLP as Functions of Nondimensional Wave Number $ka$**

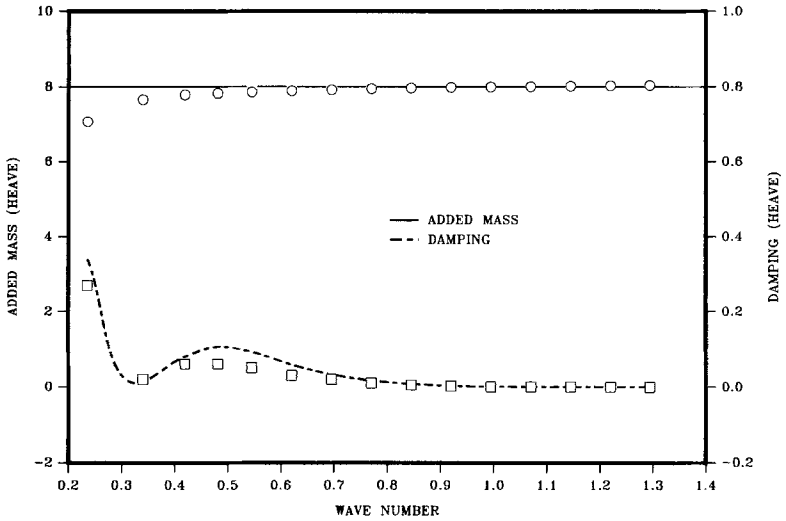


**FIG. 15. Heave-Added Mass ($\mu_{33}/\rho a^3$; ——) and Wave Damping ($b_{33}/\rho a^3\omega$; ----) for Four Columns of ISSC TLP as Functions of Nondimensional Wave Number $ka$**

In Fig. 13, the transfer function of surface amplitude along the $x$-axis $|\eta(x, 0)/A|$ for four columns (radius = 8.4 m, draft = 29.9 m, column center-to-center distance = 67.2 m) of the TLP considered in Eatock Taylor et al. (1989) is reproduced by the present method for the case; wave period = 6.1 s and wave heading = 0°. In Eatock Taylor et al. (1989), three-

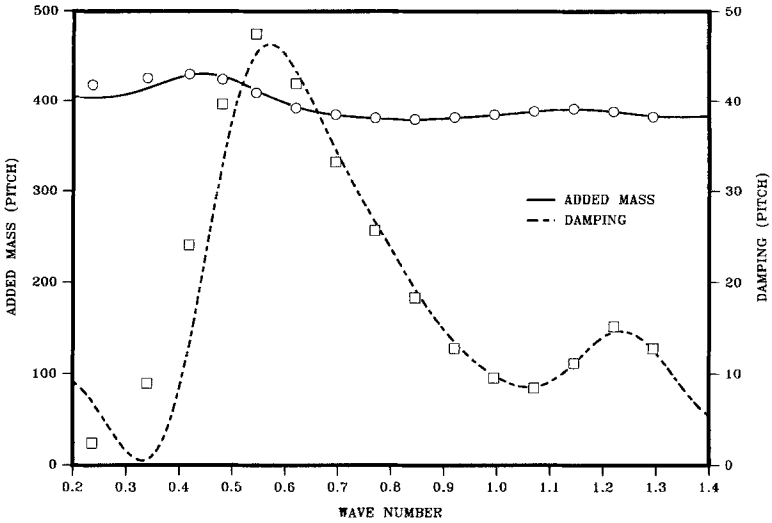


**FIG. 16. Pitch-Added Moment of Inertia ($\mu_{55}/\rho a^5$; ——) and Wave Damping ($b_{55}/\rho a^5\omega$; ----) for Four Columns of ISSC TLP as Functions of Nondimensional Wave Number $ka$**

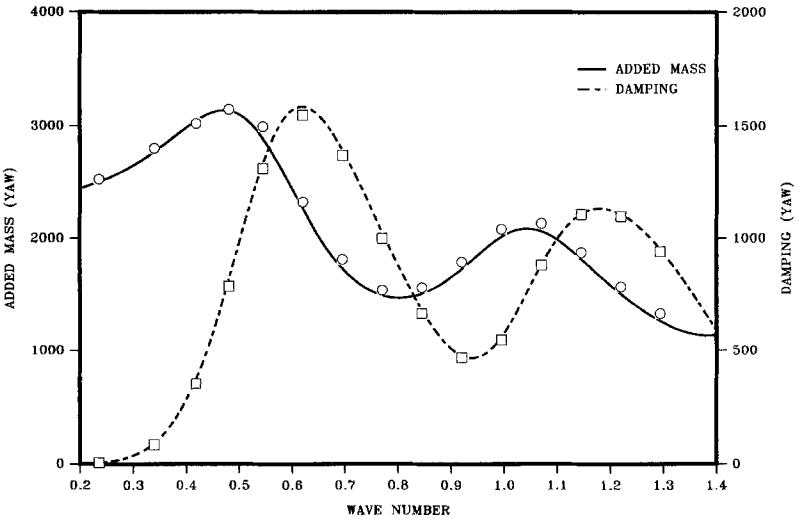


**FIG. 17. Yaw-Added Moment of Inertia ($\mu_{66}/\rho a^5$; ——) and Wave Damping ($b_{66}/\rho a^5\omega$; ----) for Four Columns of ISSC TLP as Functions of Nondimensional Wave Number $ka$**

dimensional hybrid-element approach was used to obtain the result for the full TLP including pontoons. As can be seen, good agreement is observed and this implies that the pontoons little influence the diffracted surface waves.

We next consider the radiation problem of $N$ vertical circular cylinders. In this case, the matrix equation needs to be solved not only for the fundamental wave number $k$, but also for each local wavenumber $\kappa_l$, hence the CPU time is increased accordingly. In Figs. 14–17, the added mass and

wave damping for six-degree-of-freedom motions of four cylinders of the ISSC TLP are computed by the present method and plotted as functions of nondimensional wave number $ka$. The results are compared with those calculated from the three-dimensional panel program and good agreement is observed, except at low frequencies of heave and pitch modes, where the discrepancy can be attributed to the bottom effect. In Figs. 14–17, circles and boxes represent the results computed from the three-dimensional panel program.

Due to the large draft, the heave-added mass is almost constant with frequency and the heave-wave damping is very small. As pointed out earlier, the heave-added mass and wave damping cannot be obtained directly by the present method. In this paper, the heave-added mass of a single deep cylinder is calculated by the ring-source boundary-element method (Kim and Yue 1989), and the average value of $\mu_{33}/\rho a^3$ is found to be close to two. Neglecting the mutual influence, four times of the preceding value can be used as an approximation of the actual heave-added mass of the four cylinders, as shown in Fig. 15. This bottom contribution also affects the pitch-roll added moment of inertia through its moment arm.

Although the heave-wave damping is very small and practically not important, there is a simple way of evaluating it from the combined use of Froude-Krilov heave-force approximation and Haskind relation. This result is shown in Fig. 15, and we see that the approximation reasonably predicts the actual trend. One possible way of improving the present method to better estimate heave hydrodynamic coefficients is to use additional inner eigenfunction expansions inside the radius of each cylinder (Garrett 1971; Williams and Demirbilek 1988) followed by matching the entire flow.

In Figs. 4–17, the hydrodynamic loadings on four truncated cylinders are presented in the frequency range $ka = 0.2$–$1.4$. The lowest frequency corresponds to the draft wavelength ratio, $D/L = 0.13$. The present analytic solutions are supposed to give better accuracy at higher frequencies (or shorter wavelengths). In other words, if $D/L > 0.5$, the wave cannot feel the bottom of the cylinder, hence the present solutions should be accurate. Otherwise, the present method is an approximation. From our numerical examples, it is seen that the results at low frequencies are still pretty good, except for pitch-wave damping and can be used if such an error is allowable.

## CONCLUSION

In this paper, Linton and Evans' (1990) diffraction theory originally developed for $N$ bottom-mounted vertical circular cylinders is generalized to be applicable to deep-draft truncated vertical cylinders. More importantly, the complementary analytic radiation potential, added mass, and wave damping are also derived in closed forms. The radiation problem turns out to be more complicated than Linton and Evans' (1990) diffraction formulation due to the existence of local (or evanescent) waves. Since local waves are included, the present radiation solutions can be used even when the cylinders are very closely spaced. Based on those analytic solutions, an approximate, computationally efficient method to compute hydrodynamic loads on deep truncated cylinders is developed. The results are validated through comparisons with other numerical methods. In our numerical examples, we see pronounced peaks and troughs depending on the wavelength (or the spacing of the columns), and they are very sensitive to the change of wave headings, which underscores the importance of wave directionality in such application.

The hydrodynamic loading on multicolumn structures containing a very large number of cylindrical legs can be efficiently approximated by the present method, while the use of the three-dimensional panel program in those applications could be tedious and costly. The present method quickly produces reasonably accurate solutions and precludes the laborious convergence test and grid generation. The present method is particularly useful in the preliminary design, where a parametric study with varying geometry is required.

## ACKNOWLEDGMENT

This work was conducted under a joint industry project sponsored by Shell Development Company, Chevron, Conoco USA, Mobil, and Brown & Root. The writer thanks Z. Ran for his valuable assistance in the graphics of the results.

## APPENDIX. REFERENCES

Abul-Azm, A. G., and Williams, A. N. (1988). "Second order diffraction loads on two uniform vertical cylinders." *Proc. 7th Offshore Mechanics and Arctic Engineering Symp.*, OMAE, 2, 131–138.

Chen, X. B., and Molin, B. (1990). "High frequency interactions between TLP legs." *5th Int. Workshop on Water Waves and Floating Bodies.*

Demirbilek, Z. (1989). "Tension leg platform: an overview of the concept, analysis and design." *ASCE monograph, tension leg platform*, ASCE, New York, N.Y., 1–14.

Eatock Taylor, R., and Hung, S. M. (1985). "Wave drift enhancement effects in multi-column structures." *J. Appl. Oc. Res.*, 7, 128–137.

Eatock Taylor, R., and Jefferys, E. R. (1986). "Validity of hydrodynamic load predictions for a tension leg platform." *Oc. Engrg.*, 13, 449–490.

Eatock Taylor, R., and Sincock, P. (1989). "Wave upwelling effects in TLP and semisubmersible structures." *Oc. Engrg.*, 16, 281–306.

Faltinsen, O. M., and Demirbilek, Z. (1989). "Hydrodynamic analysis of TLPs." *ASCE monograph, tension leg platform*, ASCE, New York, N.Y., 36–63.

Garrett, C. J. R. (1971). "Wave forces on a circular dock." *J. Fluid Mech.*, 46, 129–139.

Kagemoto, H., and Yue, D. K. P. (1986a). "Interactions among multiple three-dimensional bodies in water waves: an exact algebraic method." *J. Fluid Mech.*, 166, 189–209.

Kagemoto, H., and Yue, D. K. P. (1986b). "Wave forces on a platform supported on a large number of floating legs." *5th Conf. Offshore Mech. and Arctic Engrg.*, ASME, New York, N.Y.

Kim, M. H. (1991). "Second-order sum-frequency wave loads on large-volume structures." *J. Appl. Oc. Res.*, (Dec.).

Kim, M. H., and Yue, D. K. P. (1989). "The complete second-order diffraction solution for an axi-symmetric body. part 1: Monochromatic incident waves." *J. Fluid Mech.*, 200, 235–264.

Korsmeyer, F. T., Lee, C. H., Newman, J. N., and Sclavounos, P. D. (1988). "The analysis of wave effects on tension-leg platforms." *Proc., Offshore Mechanics and Arctic Engrg.*, ASME, New York, N.Y.

Linton, C. M., and Evans, D. V. (1990). "The interaction of waves with arrays of vertical circular cylinders." *J. Fluid Mech.*, 215, 549–569.

McIver, P. (1987). "Mean drift forces on arrays of bodies due to incident long waves." *J. Fluid Mech.*, 185, 469–482.

McIver, P., and Evans, D. V. (1983). "Approximation of wave forces on cylinder arrays." *J. Appl. Oc. Res.*, 6, 101–107.

Ohkusu, M. (1974). "Hydrodynamic forces on multiple cylinders in waves." *Intl. Symp. on Dynamics of Marine Vehicles and Structures in Waves.*
Spring, B. H., and Monkmeyer, P. L. (1974). "Interaction of plane waves with vertical cylinders." *Proc. 14th Conf. on Coastal Engrg.*, 1828–1845.
Williams, A. N., and Demirbilek, Z. (1988). "Hydrodynamic interactions in floating cylinder arrays 1. wave scattering." *Oc. Engrg.*, 15, 549–584.